

**Supporting Information**

**Hollow N-doped carbon nano-mushroom encapsulated hybrid Ni<sub>3</sub>S<sub>2</sub>/Fe<sub>5</sub>Ni<sub>4</sub>S<sub>8</sub> particle anchored to the inner wall of porous wood carbon for efficient oxygen evolution electrocatalysis**

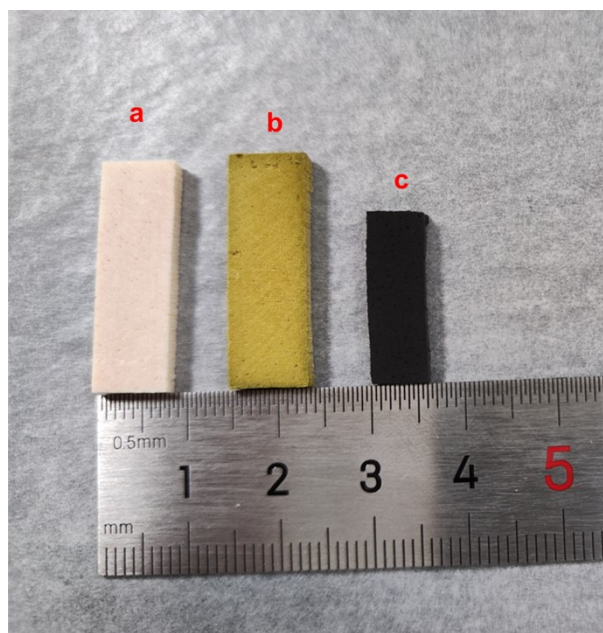
Ying Wang,<sup>1†</sup> Yuntang, Zhuang,<sup>1†</sup> Yaru Hu,<sup>1</sup> Fangong Kong,<sup>1</sup> Guihua Yang,<sup>1</sup> Orlando J. Rojas,<sup>2</sup> Ming He<sup>1,\*</sup>

<sup>1</sup>State Key Laboratory of Biobased Material and Green Papermaking, Qilu University of Technology (Shandong Academy of Sciences), Jinan, Shandong Province, 250353, P. R. China

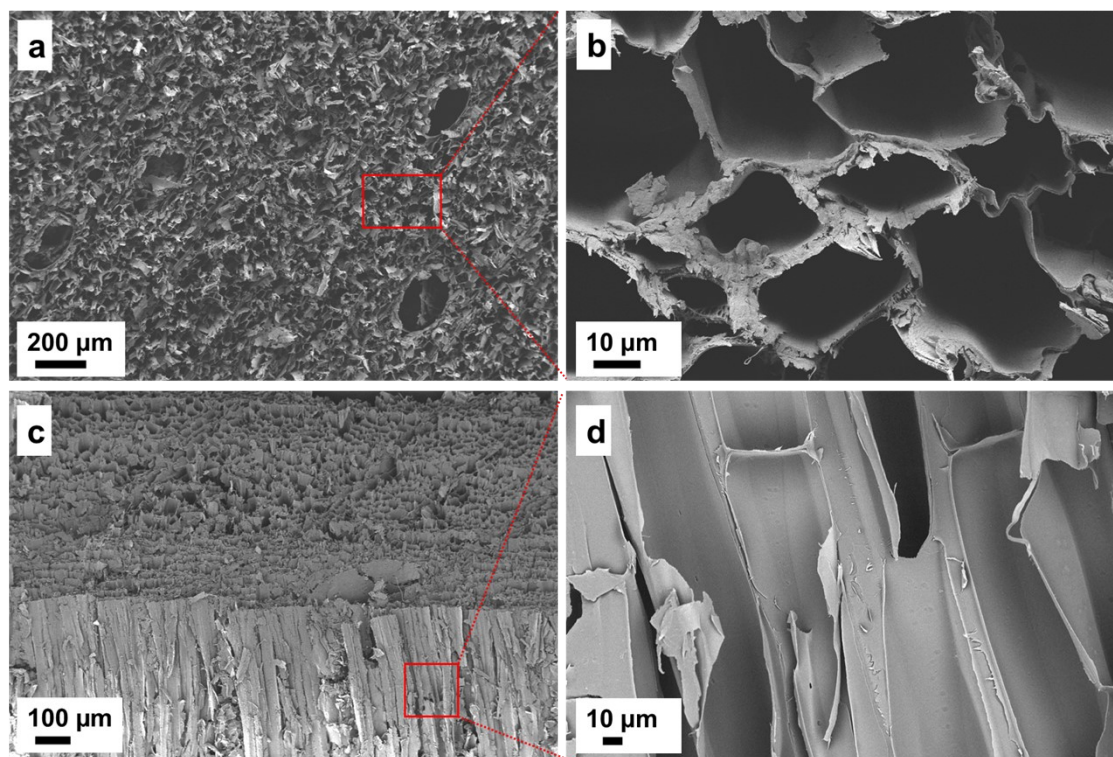
<sup>2</sup>Bioproducts Institute, Department of Chemical & Biological Engineering, Department of Chemistry and Department of Wood Science, 2360 East Mall, The University of British Columbia, Vancouver, BC V6T 1Z3, Canada

\*Corresponding author: heming8916@qlu.edu.cn (M. He)

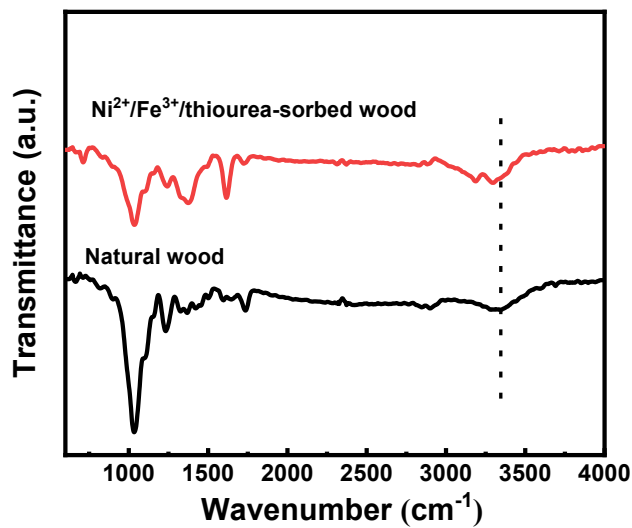
†These authors contributed equally to this work.



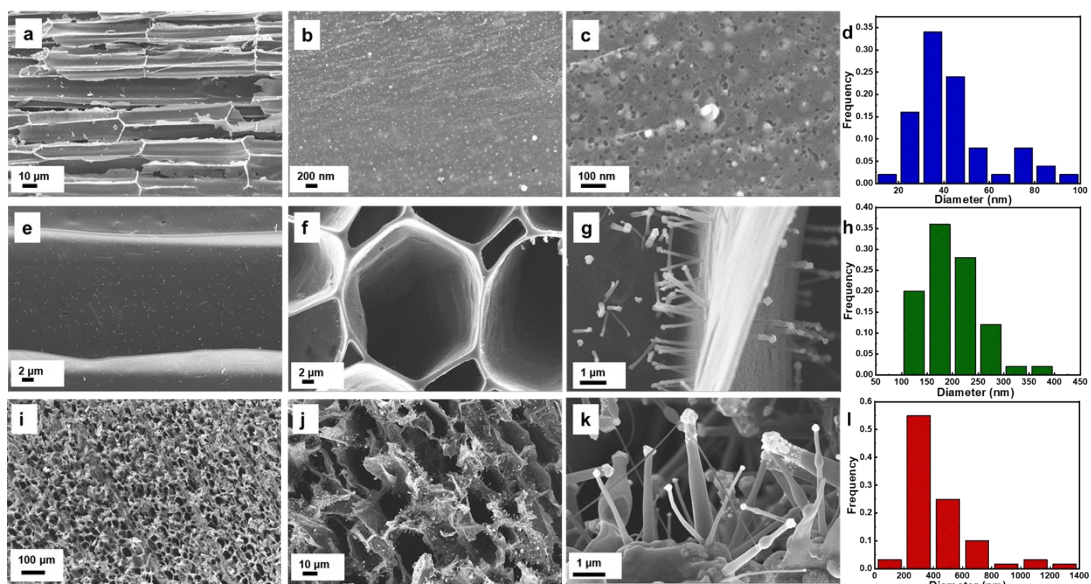
**Figure S1.** The digital photo of (a) natural balsa wood, (b) impregnated wood, and (c) NiFeS<sub>14</sub>@NCNM/CW.



**Figure S2.** SEM images on the (a, b) cross-section and (c, d) tangential-section view for balsa wood, respectively.



**Figure S3.** FTIR spectra of natural wood and  $\text{Ni}^{2+}/\text{Fe}^{3+}$ /thiourea-sorbed wood, respectively.



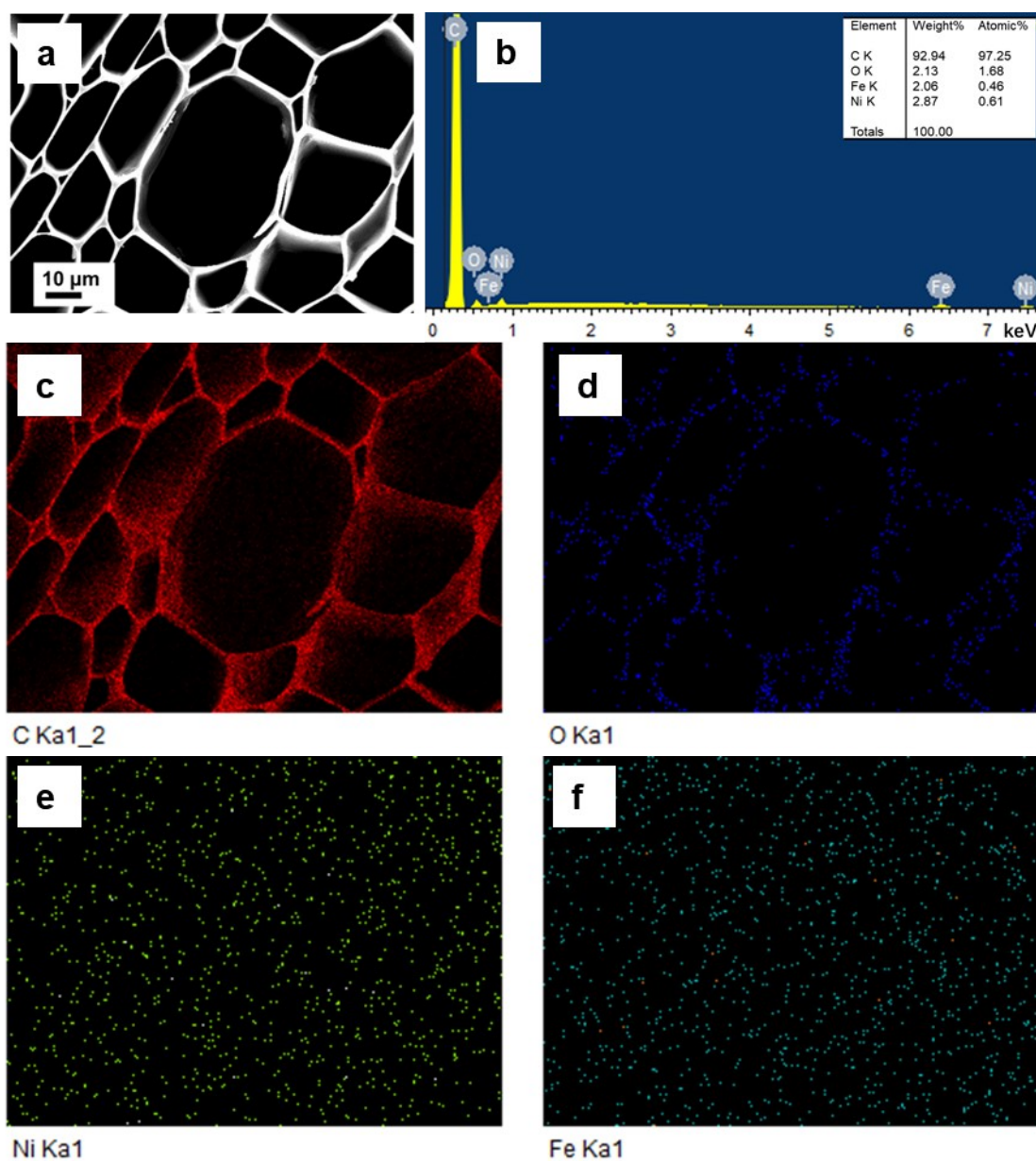


**Figure S5.** (a) Representative SEM image, (b) the corresponding EDX spectrum, and (c-f) element mapping of NiFe/CW.

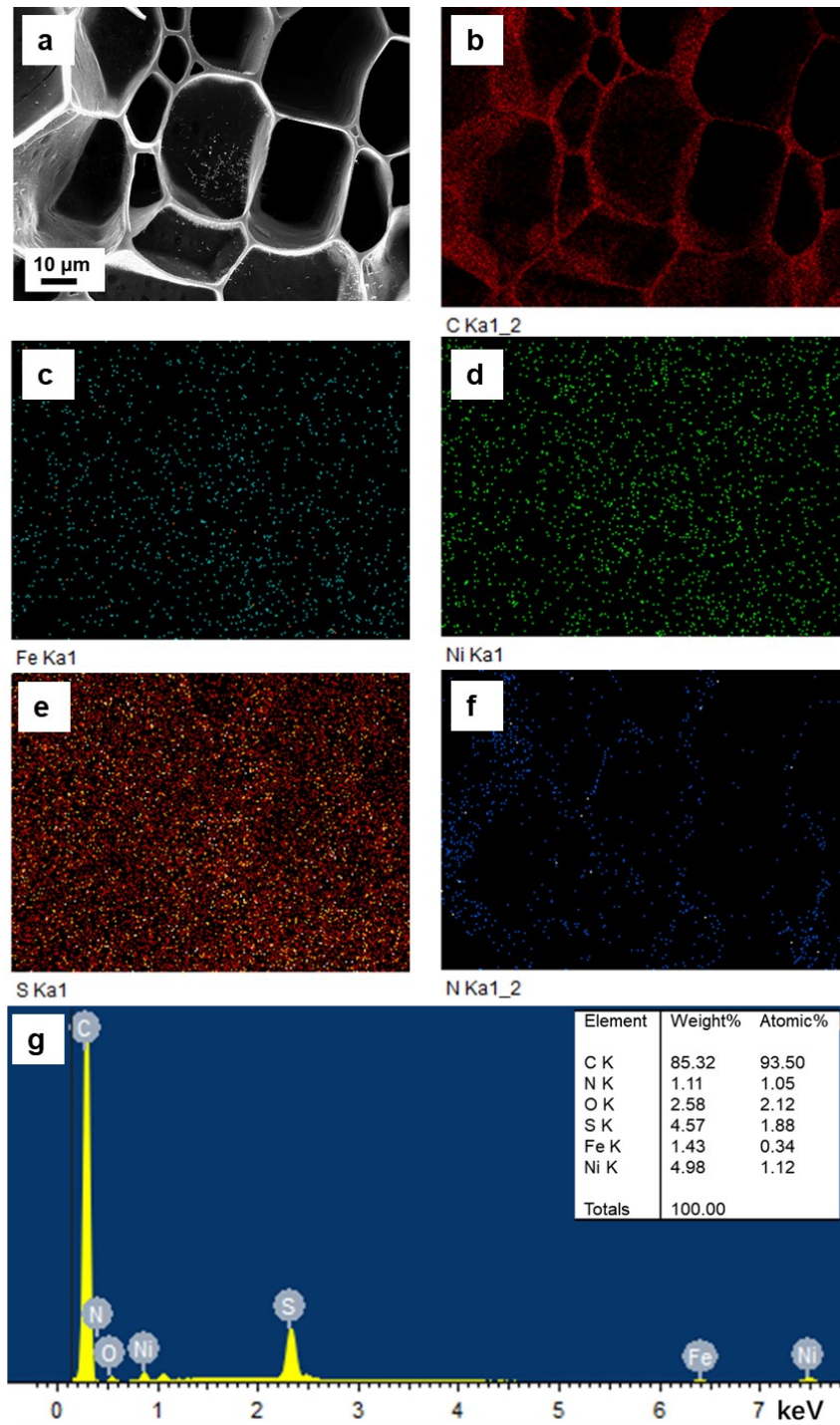


**Figure S6.** (a) Representative SEM image, (b-f) element mapping, and (g) the corresponding EDX spectrum of NiFeS8@NCNM/CW.

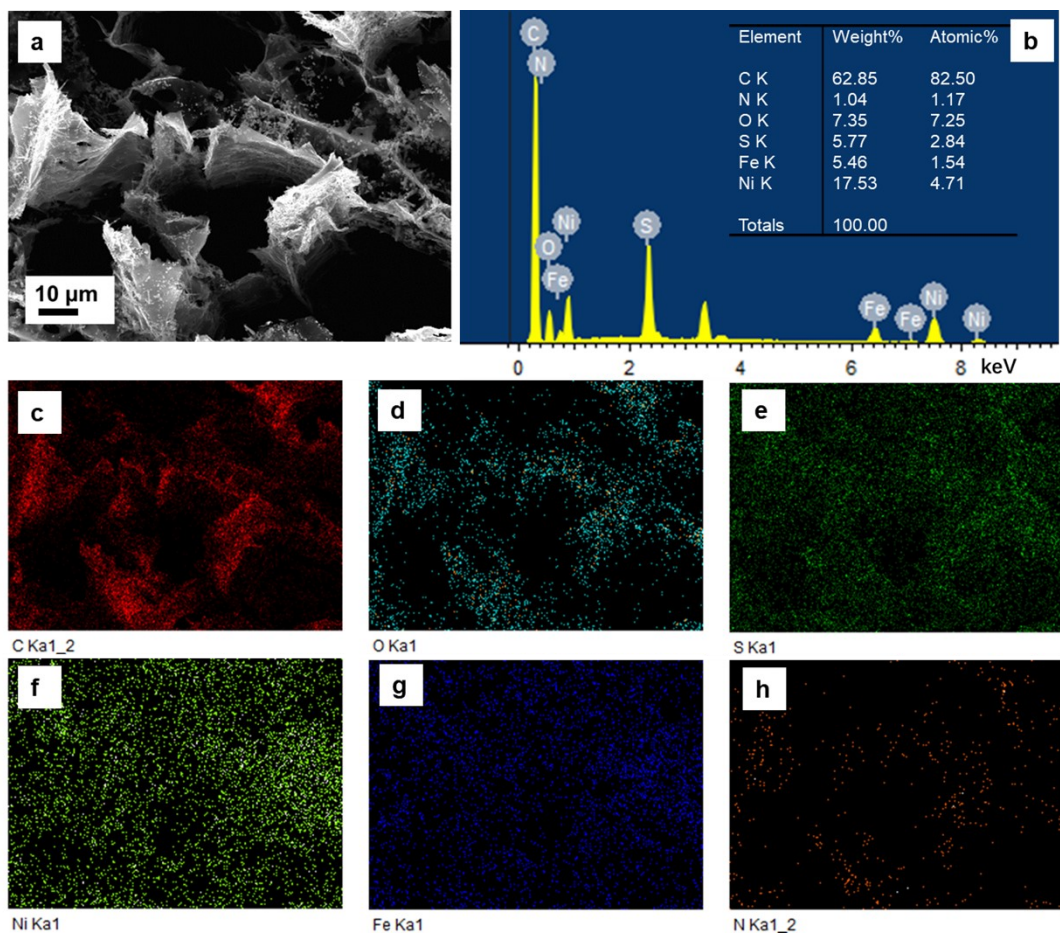


**Figure S7.** (a) Representative SEM image, (b) the corresponding EDX spectrum, and (c-h) element mapping of NiFeS<sub>14</sub>@NCNM/CW.

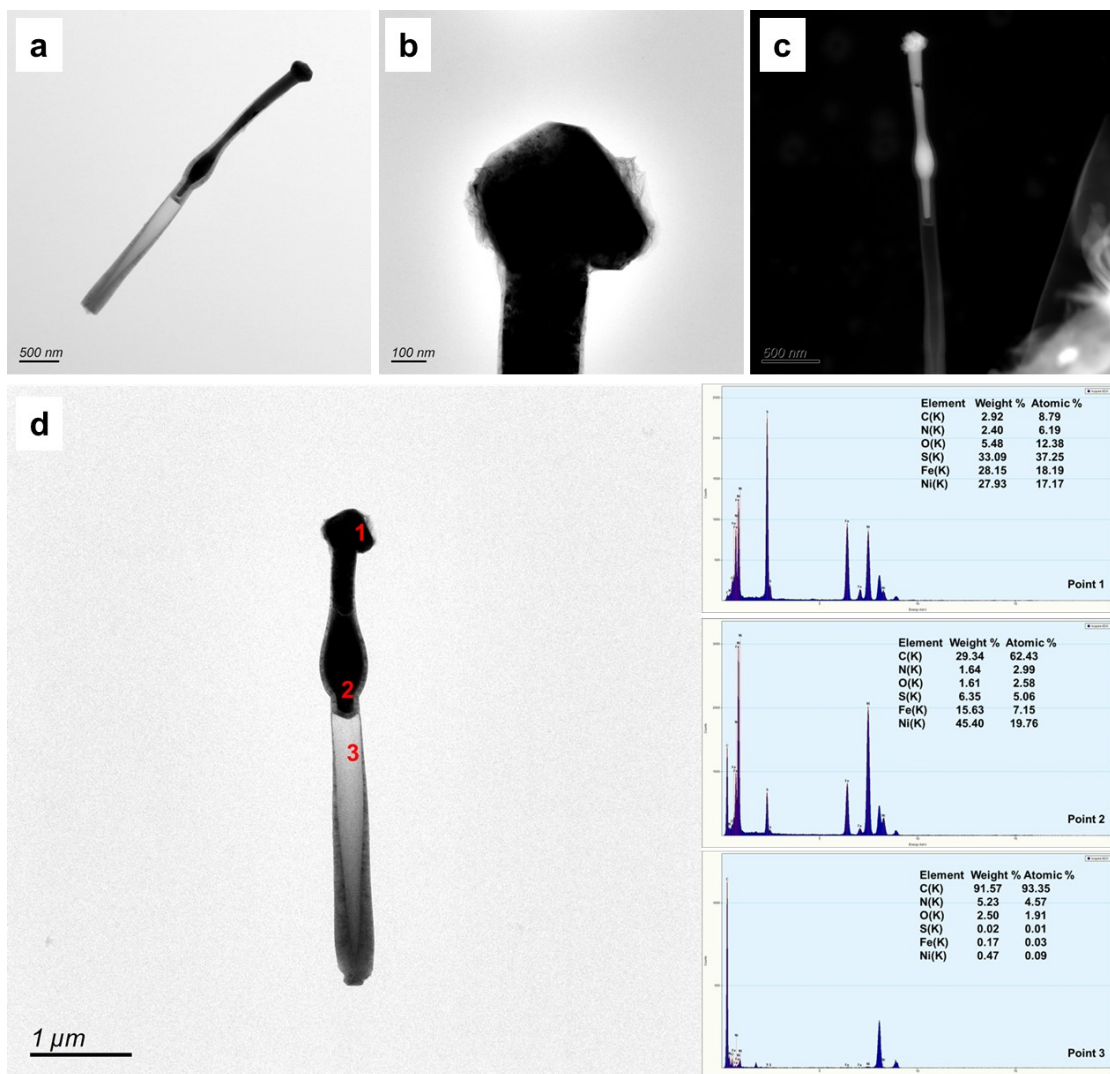


**Figure S8.** (a, b) TEM, (c) HAADF-STEM images, and (d) EDX spectra corresponding to different points of NiFeS<sub>14</sub>@NCNM/CW.

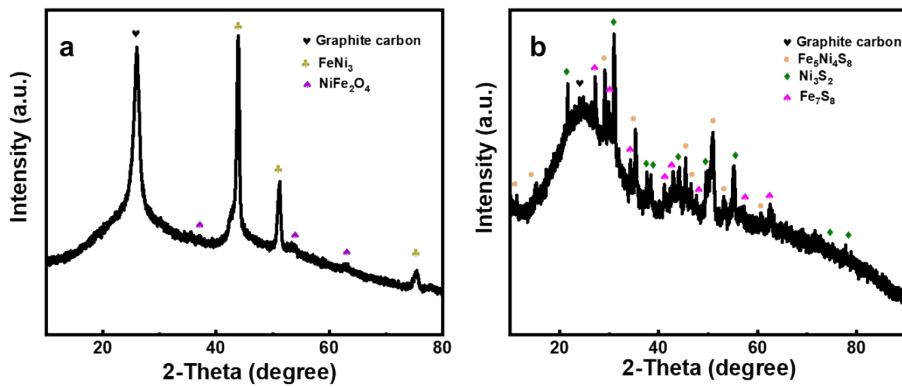


**Figure S9.** XRD patterns of the (a) NiFe/CW and (b) NiFeS8@NCNM/CW.

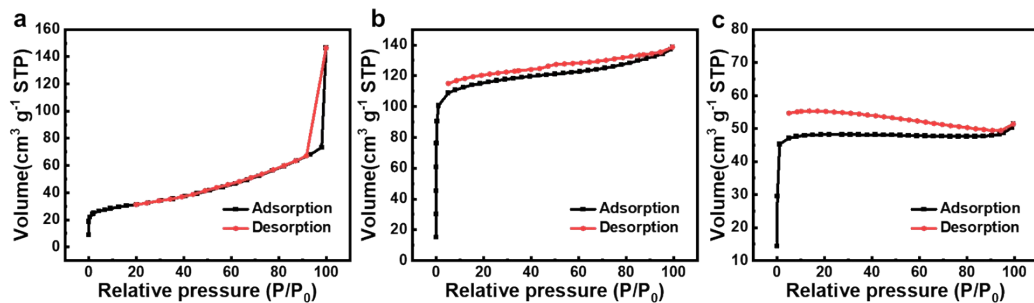


**Figure S10.** Nitrogen adsorption-desorption isotherms of (a) NiFeS8@NCNM/CW, (b) NiFe/CW, and (c) CW.

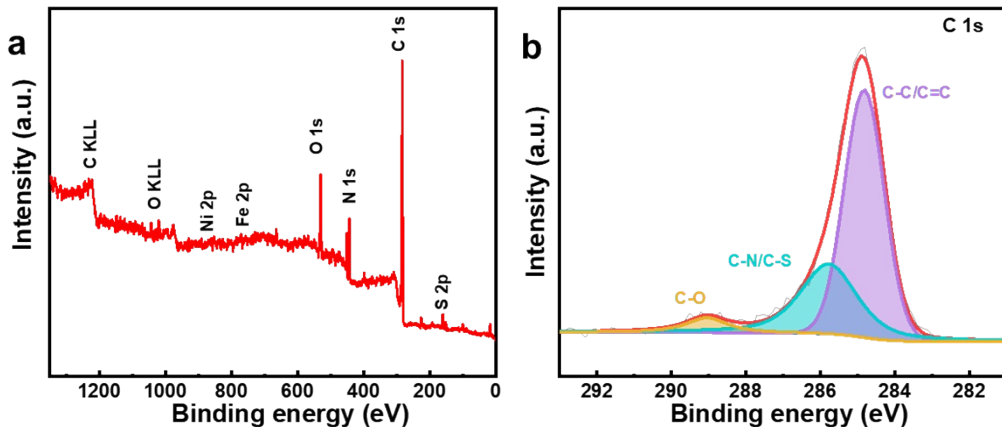


**Figure S11.** (a) Full XPS spectrum and (b) C 1s high-resolution spectrum of NiFeS14@NCNM/CW.

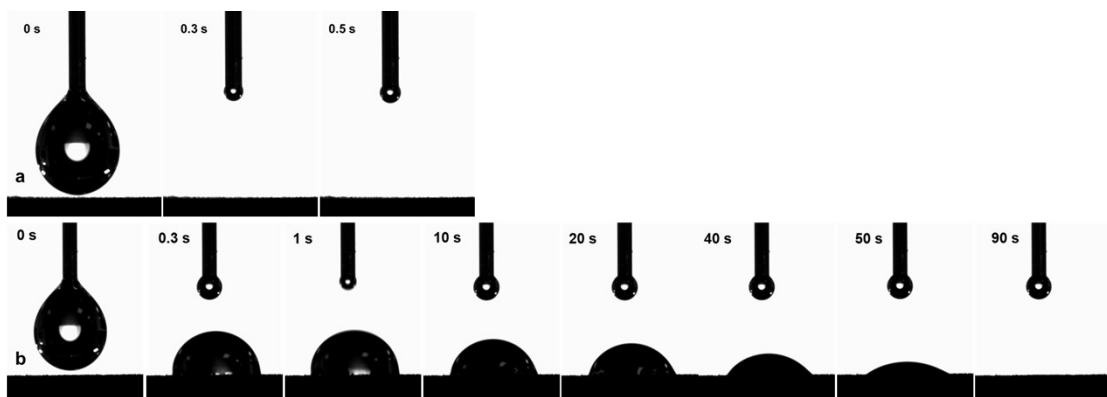


**Figure S12.** Static-water-droplet contact angles for (a) NiFeS14@NCNM/CW and (b) CW.

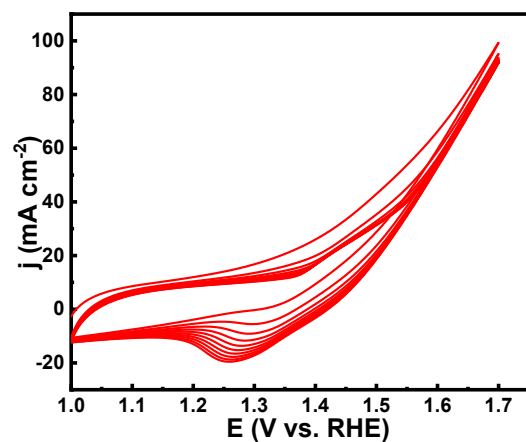


**Figure S13.** The whole activation CV curves of NiFeS14@NCNM/CW with the scan rate of  $50 \text{ mV s}^{-1}$ .

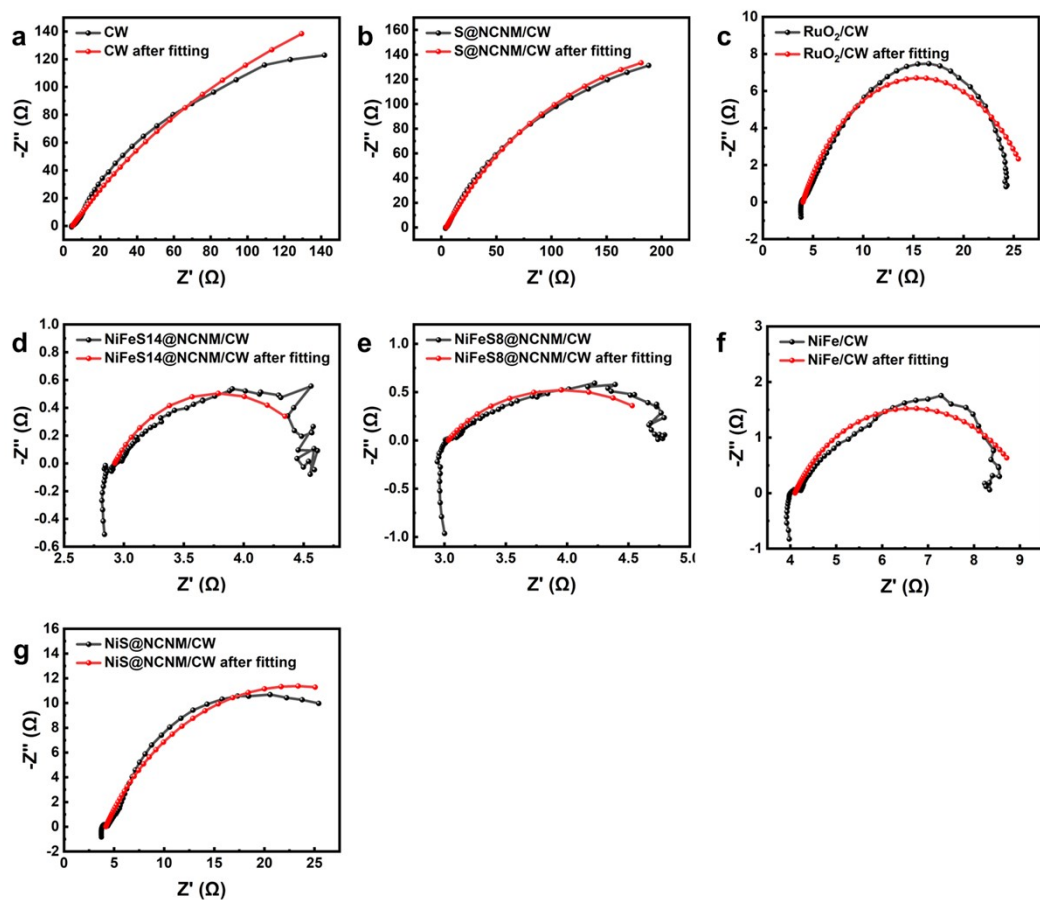


**Figure S14.** The original and the as-fitted Nyquist plots of different catalysts.

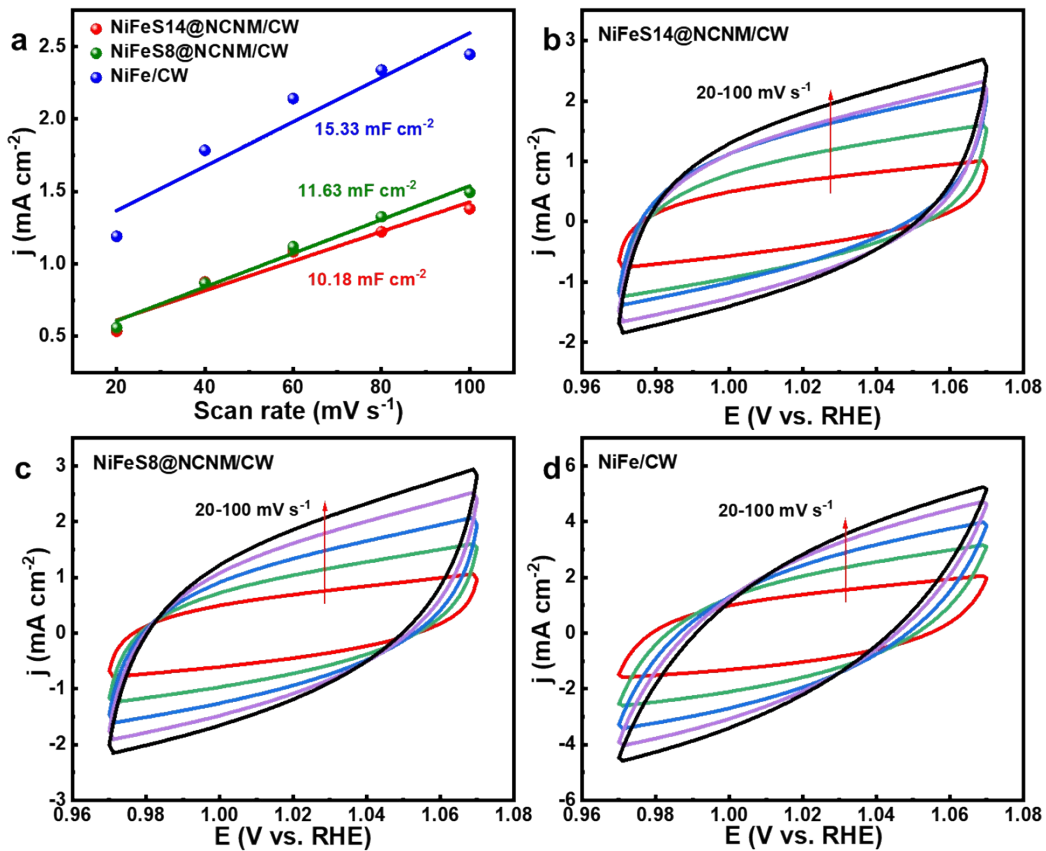


**Figure S15.** (a) The capacitive currents at 1.02 V vs. RHE as a function of scan rate for different catalysts. CV profiles of (b) NiFeS14@NCNM/CW, (c) NiFeS8@NCNM/CW, and (d) NiFe/CW with different scan rates of 20, 40, 60, 80, 100  $\text{mV s}^{-1}$ .

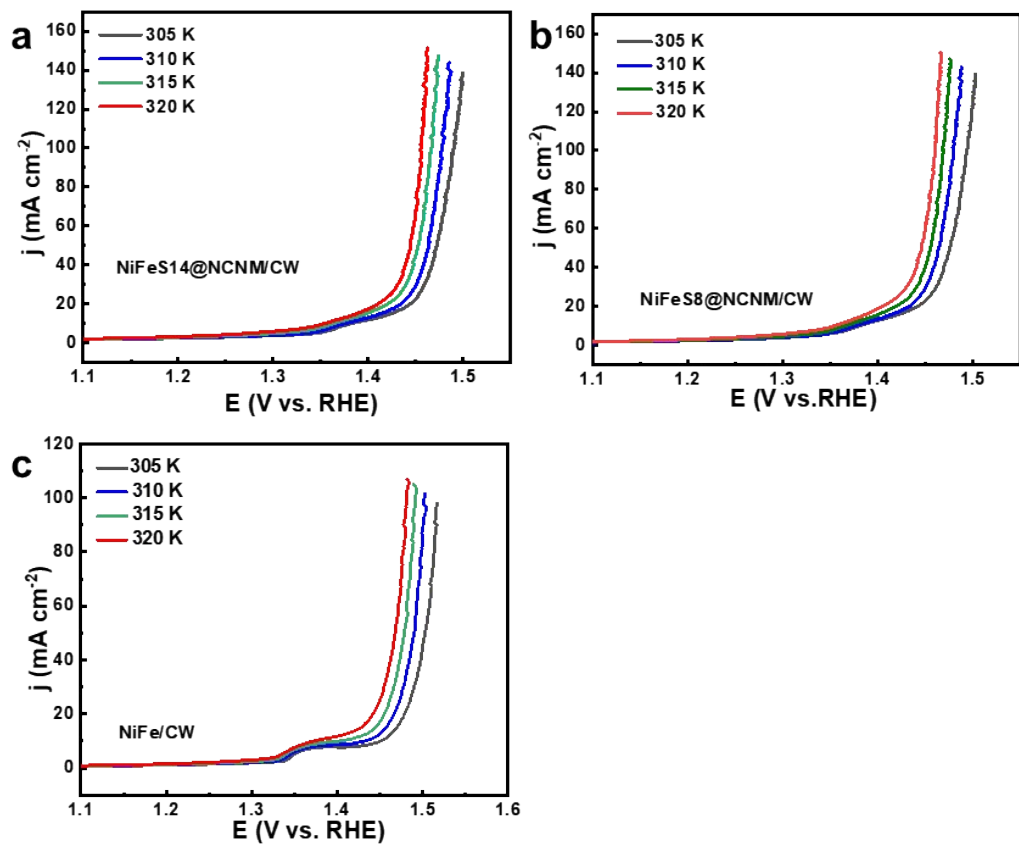


**Figure S16.** OER polarization curves of the (a) NiFeS<sub>14</sub>@NCNM/CW, (b) NiFeS<sub>8</sub>@NCNM/CW, and (c) NiFe/CW in 1 M KOH at different temperatures.

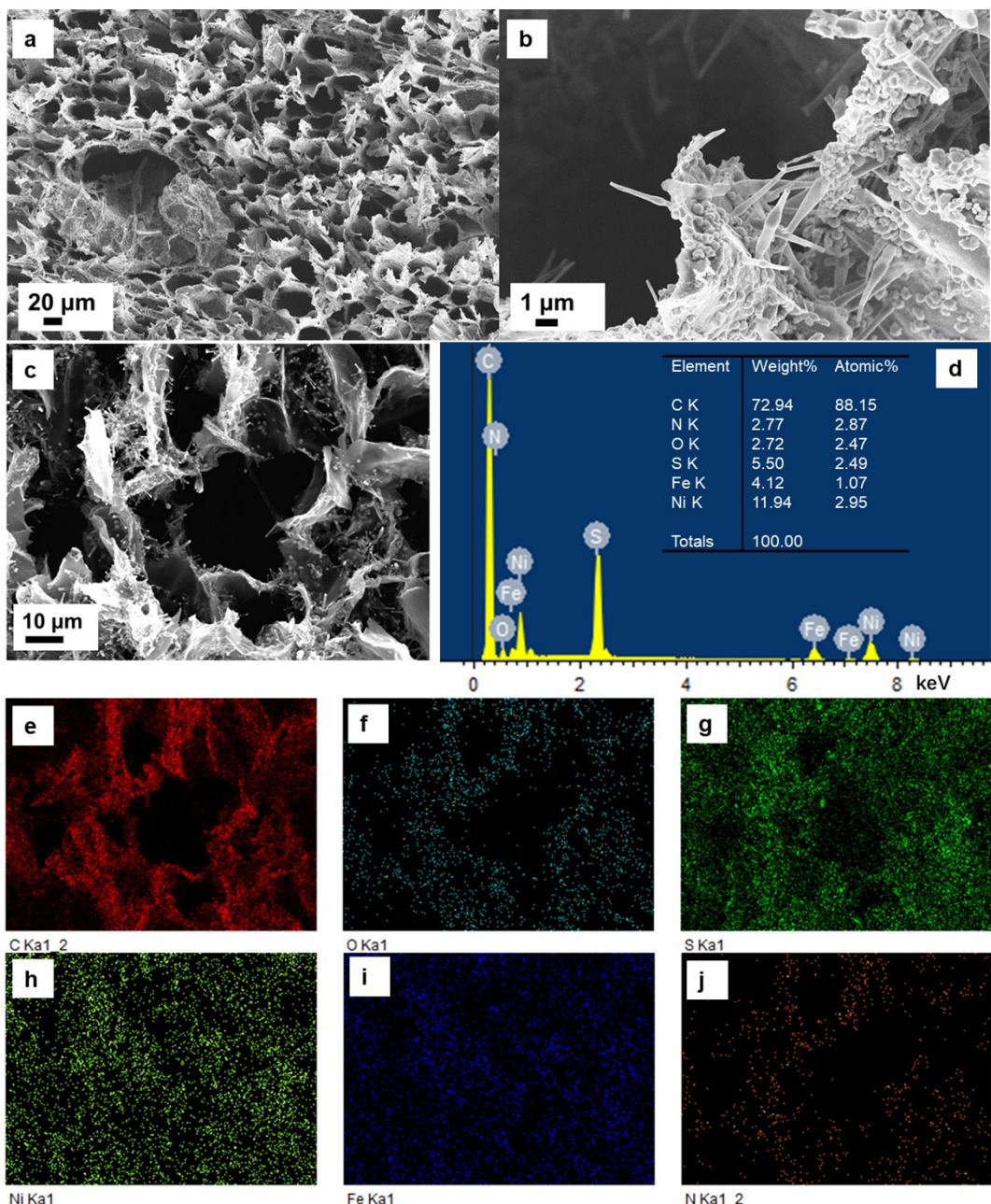


**Figure S17.** (a-c) Representative SEM images, (d) the corresponding EDX spectrum, and (e-j) EDX mapping of NiFeS<sub>14</sub>@NCNM/CW after durability test.

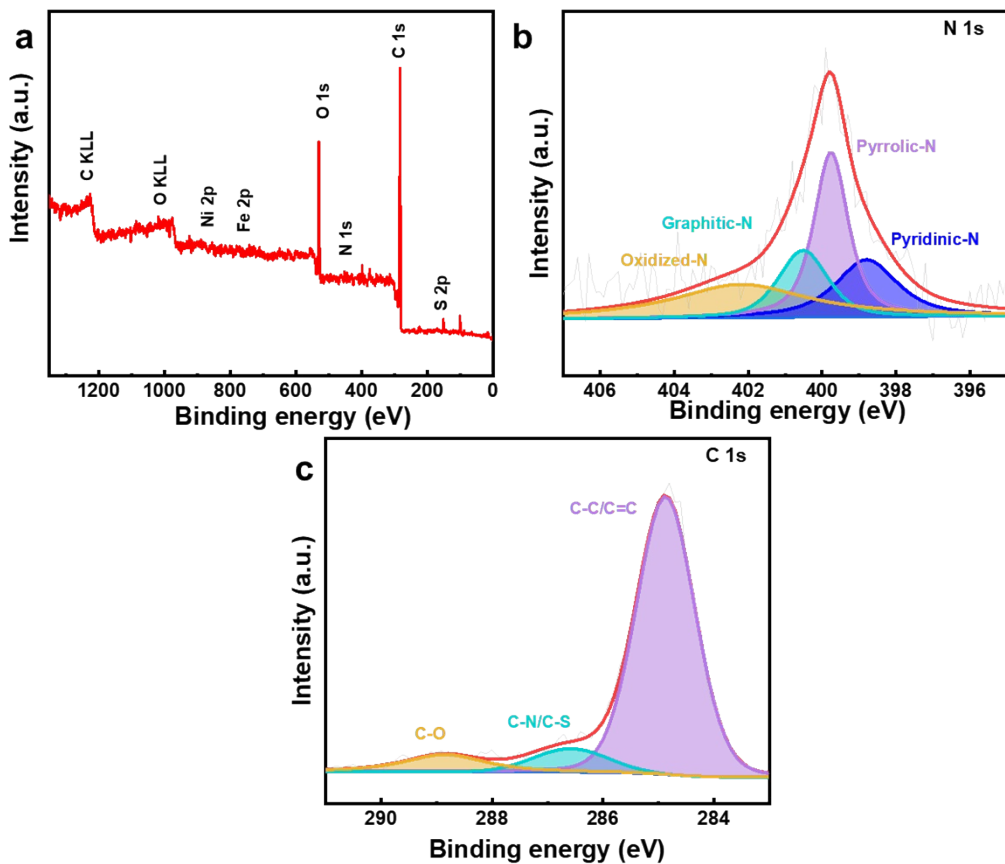


**Figure S18.** (a) Full XPS spectrum, (b) N 1s, and (b) C 1s high-resolution XPS spectra of NiFeS<sub>14</sub>@NCNM/CW after the OER durability test.

**Table S1.** Comparisons of OER activities of NiFeS14@NCNT/CW with those of recently reported biomass-derived carbon-supported electrocatalysts.

Catalyst	Carbon source	$\eta_{10}$ (mV)	Tafel (mV dec <sup>-1</sup> )	Stability(i-t)	Refs.
<b>147@10</b>					
NiFeS14@NCNM/CW	balsa wood	mA cm <sup>-2</sup> 250@50	56.3	retain 93% after 24 h	This work
Co/Ni-CW	basswood	330	68	retain 92% after 10 h	<sup>1</sup>
Co@N-HPMC	basswood	297	115.7	retain 64% after 3 h	<sup>2</sup>
Ni-W-B/wood	fir wood	360@50	86.3	retain 90.4% after 50 h	<sup>3</sup>
Co@NCW	paulownia wood	350	92	stable after 10 h	<sup>4</sup>
CoFe@NC/WC	spruce wood	315	57.6	stable after 24 h	<sup>5</sup>
NiFe/DWC	poplar wood	260@100	98	potential retain 97% after 60 h	<sup>6</sup>
Co@NCW	basswood	410	-	-	<sup>7</sup>
Ni <sub>3</sub> Fe-CW	basswood	237	138	retain 94.6% after 50 h	<sup>8</sup>
FeNiP@NCNT/CW	balsa wood	180@50	60.9	retain 96% after 200 h	<sup>9</sup>
N/E-HPC-900	eucalyptus wood	440	-	retain 90% after 5.6 h	<sup>10</sup>
FeNi <sub>3</sub> @NC	chitosan	277	77	retain ~90% after 10 h	<sup>11</sup>
CCC-PAN	cotton cloth	351	135	retain 85% after 15 h	<sup>12</sup>
NPCNS	leaves	340@5	191	retain 83.6% after 20 h	<sup>13</sup>
Co <sub>9</sub> S <sub>8</sub> @Co-N/C	tissue paper	373	78.4	-	<sup>14</sup>
Fe <sub>3</sub> O <sub>4</sub> /NiS@CC	Cotton cloth	310	82	stable after 26 h	<sup>15</sup>

**Table S2.** Electrochemical impedance parameters obtained simulating the Nyquist plots in Figure 5f to the equivalent circuit model.

Catalyst	R <sub>s</sub>	R <sub>ct</sub>	CPE-T	CPE-P
NiFeS14@NCNM/CW	2.923	1.739	0.2194	0.66882
NiFeS8@NCNM/CW	3.031	1.856	0.21129	0.6518
NiFe /CW	4.104	5.066	0.11518	0.69006
RuO <sub>2</sub> /CW	3.994	23.17	0.024906	0.66823
NiS@NCNM/CW	4.179	37.91	0.15231	0.68815
S@NCNM/CW	4.517	505.1	0.019479	0.65664
CW	4.878	671.7	0.030537	0.69094

## References

1. W. Gan, L. Wu, Y. Wang, H. Gao, L. Gao, S. Xiao, J. Liu, Y. Xie, T. Li and J. Li, *Adv. Funct. Mater.*, 2021, **31**, 2010951.
2. Y. Li, S. Min and F. Wang, *Sustain. Energ. Fuels*, 2019, **3**, 2753-2762.
3. L. Chen, J. Zhang, B. Lu, H. Liu, R. Wu and Y. Guo, *Int. J. Hydrogen Energy*, 2022, **47**, 35571-35580.
4. Y. Wang, K. Sheng, R. Xu, Z. Chen, K. Shi, W. Li and J. Li, *Chem. Eng. Sci.*, 2023, **268**, 118433.
5. K. Ao, X. Zhang, R. R. Nazmutdinov, D. Wang, J. Shi, X. Yue, J. Sun, W. Schmickler and W. A. Daoud, *Energy Environ. Mater.*, 2023, **0**, e12499.
6. Y. Huang, Y. Qing, Y. Chen, Y. Liao, A. Jiang, Y. Li, Y. Wu, C. Tian and N. Yan, *ACS Sustainable Chem. Eng.*, 2022, **10**, 15233-15242.
7. W. Li, F. Wang, Z. Zhang and S. Min, *Appl. Catal., B*, 2022, **317**, 121758.
8. Y. Wang, Y. Shang, Z. Cao, K. Zeng, Y. Xie, J. Li, Y. Yao and W. Gan, *Chem. Eng. J.*, 2022, **439**, 135722.
9. X. Tao, H. Xu, S. Luo, Y. Wu, C. Tian, X. Lu and Y. Qing, *Appl. Catal., B*, 2020, **279**, 119367.
10. X. Peng, L. Zhang, Z. Chen, L. Zhong, D. Zhao, X. Chi, X. Zhao, L. Li, X. Lu, K. Leng, C. Liu, W. Liu, W. Tang and K. P. Loh, *Adv. Mater.*, 2019, **31**, e1900341.
11. D. Chen, J. Zhu, X. Mu, R. Cheng, W. Li, S. Liu, Z. Pu, C. Lin and S. Mu, *Appl. Catal., B*, 2020, **268**, 118729.
12. C. Zhang, S. Bhoyate, M. Hyatt, B. L. Neria, K. Siam, P. K. Kahol, M. Ghimire, S. R. Mishra, F. Perez and R. K. Gupta, *Surf. Coat. Technol.*, 2018, **347**, 407-413.
13. Y. Huang, D. Wu, D. Cao and D. Cheng, *Int. J. Hydrogen Energy*, 2018, **43**, 8611-8622.
14. I. S. Amiinu, Z. Pu, D. He, H. G. R. Monestel and S. Mu, *Carbon*, 2018, **137**, 274-281.
15. S. Jiang, H. Shao, G. Cao, H. Li, W. Xu, J. Li, J. Fang and X. Wang, *J. Mater.*

